Exploring the Function of Tyr83 in Bacteriorhodopsin: Features of the Y83F and Y83N Mutants†

Eleonora S. Imasheva,‡ Miao Lu,‡ Sergei P. Balashov,‡ Thomas G. Ebrey,*,§ Yumei Chen,|| Zsolt Ablonczy,|| Donald R. Menick,|| and Rosalie K. Crouch||

Department of Biochemistry, University of Illinois at Urbana−Champaign, Urbana, Illinois 61801, Departments of Botany and Zoology, University of Washington, Seattle, Washington 98195, and Department of Ophthalmology, Medical University of South Carolina, Charleston, South Carolina 29425

Received May 17, 2001; Revised Manuscript Received September 6, 2001

ABSTRACT: Tyrosine-83, a residue which is conserved in all halobacterial retinal proteins, is located at the extracellular side in helix C of bacteriorhodopsin. Structural studies indicate that its hydroxyl group is hydrogen bonded to Trp189 and possibly to Glu194, a residue which is part of the proton release complex (PRC) in bacteriorhodopsin. To elucidate the role of Tyr83 in proton transport, we studied the Y83F and Y83N mutants. The Y83F mutation causes an 11 nm blue shift of the absorption spectrum and decreases the size of the absorption changes seen upon dark adaptation. The light-induced fast proton release, which accompanies formation of the M intermediate, is observed only at pH above 7 in Y83F. The pK_a of the PRC in M is elevated in Y83F to about 7.3 (compared to 5.8 in WT). The rate of the recovery of the initial state (the rate of the O → BR transition) and light-induced proton release at pH below 7 is very slow in Y83F (ca. 30 ms at pH 6). The amount of the O intermediate is decreased in Y83F despite the longer lifetime of O. The Y83N mutant shows a similar phenotype in respect to proton release. As in Y83F, the recovery of the initial state is slowed several fold in Y83N. The O intermediate is not seen in this mutant. The data indicate that the PRC is functional in Y83F and Y83N but its pK_a in M is increased by about 1.5 pK units compared to the WT. This suggests that Tyr83 is not the main source for the proton released upon M formation in the WT; however, Tyr83 is involved in the proton release affecting the pK_a of the PRC in M and the rate of proton transport from Asp85 to PRC during the O → bR transition. Both the Y83F and the Y83N mutations lead to a greatly decreased functionality of the pigment at high pH because most of the pigment is converted into the inactive P480 species, with a pK_a 8−9.

Bacteriorhodopsin (BR)[1] is a relatively small retinal protein of 26 kDa which is engaged in light-driven transmembrane proton translocation to supply the *Halobacterium* cell with energy in the form of an electrochemical potential of hydrogen ions (*1*−*3*). The retinal chromophore is attached to the protein via a protonated Schiff base linkage with Lys216. The chromophore is surrounded by the seven transmembrane α-helices of the protein and so is buried inside the transmembrane portion of the pigment (*4*). In the initial state of the pigment, the Schiff base is protonated. The positively charged Schiff base is stabilized by a complex counterion which includes negatively charged Asp85 and Asp212, positively charged Arg82, and bound water molecules (*5*−*7*). The energy of the absorbed quantum is converted into unidirectional proton translocation during the light-induced cycle of transformations of BR. This cycle involves formation and decay of several intermediate states BR → K ↔ L ↔ M_1 ↔ M_2 ↔ N ↔ O → BR (*8*−*15*). Photoisomerization of the chromophore in the primary light reaction, BR → K, and subsequent relaxation of the protein in the K → L transition (*9*), leads to a decrease of the proton affinity of the Schiff base and an increase of the affinity of Asp85 (*15*−*18*). As a result of these internal changes, the proton is transported from the Schiff base to Asp85 during the L to M transition (*19*, *20*). Almost simultaneously with this internal proton transport, another proton is released to the surface of BR (*21*−*23*), from the so-called proton release complex (PRC) which probably is a set of interacting residues including Glu204 (*24*), Glu194 (*25*, *26*), and possibly other residues and water molecules (*27*−*30*).

Spectroscopic studies of site-directed mutants and recent advances in crystallization (*31*) and determination of structure of BR (*7*, *32*) and of its M intermediate (*33*, *34*) have provided vital information on the participation of individual residues in the light-induced proton transport in BR and on structural changes underlying transmembrane proton transport. Figure 1 A depicts a fragment of hydrogen-bonded network on the extracellular side of BR based on the coordinates of Luecke et al. (*7*). Two sets of hydrogen bonds connecting Asp85 to the extracellular surface involve several residues (Asp212, Tyr57, Arg82, Glu204, Glu194, and

† This work was supported by NIH grant GM52023 (to T.G.E. and S.P.B.) and an unrestricted grant from Research to Prevent Blindness to the Department of Ophthalmology, MUSC.

* To whom correspondence should be addressed. Phone: (206) 685-3550. Fax: (206) 543-3262. E-mail: tebrey@u.washington.edu.

‡ University of Illinois at Urbana−Champaign.

§ University of Washington.

|| Medical University of South Carolina.

[1] Abbreviations: BR, bacteriorhodopsin; PRC, proton release complex.

10.1021/bi0110138 CCC: $20.00
Published on Web 10/13/2001

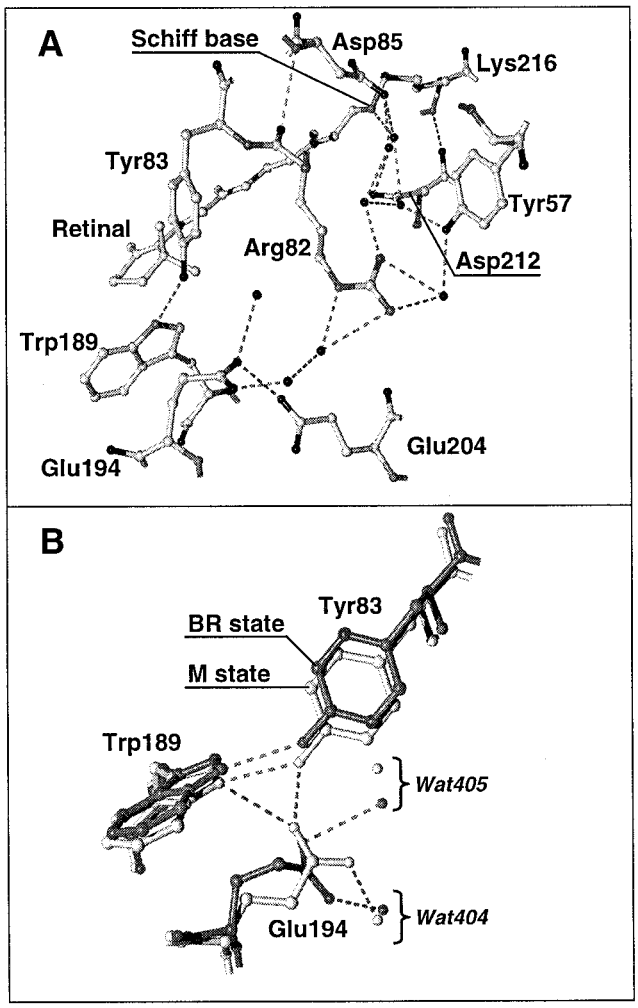

FIGURE 1: (A) Fragment of hydrogen bonded network on the extracellular domain of the ground state of BR based on the coordinates by Luecke et al. (PDB ID 1c3w) (*7*). Dotted lines represent hydrogen bonds. (B) Hydrogen bonding of Tyr83 in the BR state and in the M state of the D96N mutant based on the coordinates by Luecke et al. (PDB ID 1c8r and 1c8s, respectively) (*33*). In the BR state Tyr83 forms a hydrogen bond with Trp189. In the M state, an additional hydrogen bond between Tyr83 and Glu194 forms.

others) and water molecules. The system of hydrogen bonds undergoes light-induced rearrangements involving substantial movement of the side chain of Arg82 (*33*, *34*). This movement is likely to be at least partly responsible for the coupling of protonation states of Asp85 and the PRC. This coupling was established for wild-type BR (*27*, *35*) and several mutants (*17*, *36*), but is absent or dramatically decreased in the R82A/Q (*35*, *37*), E204Q/N (*36*, *37*) and E194C/Q mutants (*25*, *26*, *36*). Fast light-induced proton release is absent in these mutants at neutral pH. This implicates the Glu204, Glu194, and Arg82 residues as key components of the PRC (*25*, *26*, *28*, *29*). However, the exact source of a proton released upon M formation and protonation of Asp85 remains uncertain.

In this paper, we investigated the Y83F and Y83N mutants. Tyr83 is a residue conserved throughout the halobacterial family of retinal proteins (*38*) and in proteorhodopsin, a recently discovered retinal protein homologous to BR capable of light-driven proton pumping in marine *Proteobacteria* (*39*). According to the X-ray structures in BR, it is located at the extracellular domain in helix C. The hydroxyl group of Tyr83 is hydrogen bonded to Trp189 in helix F (*7*, *32*, *34*) and is in the vicinity of Glu194 in the initial unphotolyzed state of BR. Moreover, the hydroxyl of Tyr83 makes a hydrogen bond with Glu194 when the pigment is transformed into the M intermediate (*33*, *34*) (Figure 1 B). This suggests that Tyr83 might be involved in proton release. To check the consequences of eliminating the hydroxyl group of Tyr83, we studied properties of the mutants in which tyrosine 83 was substituted with phenylalanine and asparagine (the Y83F and Y83N mutants). We examine the kinetics of light-induced proton release and other features of the mutants that provide information on the PRC and its interaction with primary proton acceptor Asp85 (*15*, *27*). These are the pH dependencies of absorption spectra and of the rate constant of dark adaptation (thermal all-trans → 13-cis isomerization of the chromophore) and the pH dependencies of formation of the M intermediate. We found that fast proton release is strongly affected by the Y83 mutations though it can be observed at high pH. The coupling of Asp85 and PRC is decreased in the Y83F and Y83N mutants, which results in the increase of the pK_a of PRC by about 1.5 pK_a units in M. The rate of initial pigment recovery is slowed several fold. Data indicate the importance of hydroxyl group of Tyr83 in efficient functioning and stability of BR.

MATERIALS AND METHODS

The construction and expression of the Y83F and Y83N mutants *in Halobacterium salinarum* were accomplished following methods described earlier (*17*, *35*). The identity of the mutants was confirmed by mass spectrometry. The preparation of the BR samples and their analysis were performed by the methods developed earlier for the mass spectrometric analysis of integral membrane proteins (*40*). The preparation process involved hexanes−ethanol delipidation of the BR membranes and cleavage with cyanogen bromide. The cleavage mixture was then separated with high-performance liquid chromatography (HPLC) and analyzed online with a Finnigan LCQ Ion Trap Mass Spectrometer. The absorption spectra were recorded on a Cary-Aviv 14DS spectrophotometer (Aviv Associates, Lakewood, NJ). The pH titration, dark adaptation, and flash photolysis experiments were performed as described in our earlier studies (*17*, *35*, *36*). Purple membranes were suspended in 150 mM KCl or 75 mM K_2SO_4 (as specified in figure legends). To maintain the pH of the sample and to keep buffer capacity constant all over the pH range between pH 2 and 11, a mixture of six buffers (citric acid, Mes, Mops, Tricine, Ches and Caps) was used. Concentration of each buffer was 5 mM. The kinetics of light-induced proton release and uptake in suspensions of membranes containing the Y83F or Y83N mutants were measured with pH sensitive dye pyranine as in earlier studies (*35*, *41*). No buffer was added to the samples for measurements of light-induced proton release and uptake. The signal was obtained as a difference between traces at 458 nm in the presence and the absence of the dye. The concentration of the dye was 25 μM at pH 7.3 (pK_a of pyranine). At pH 6.3, 4−5-fold more pyranine was added. The absorbance of purple membrane at the maximum was 0.5. The dilution upon addition of the dye was insignificant (less than 1%).

RESULTS

Purple to Blue Transition in the Y83F and Y83N Mutants. Upon decreasing the pH from 7 to 2, the absorption maximum of dark-adapted wild-type BR undergoes a red shift from 558 nm to ca. 605 nm (the purple to blue transition) (*42*, *43*) caused primarily by the protonation of Asp85 (*20*) with a pK_a of 2.6 in 150 mM salt (*27*). Upon decreasing the pH from 2 to 0, in the presence of chloride ions, the absorption maximum blue shifts to 565 nm. The spectrum of this species, acid purple, is close to that of the BR (*42*, *43*). In the absence of chloride, a smaller 20 nm blue shift is observed with a pK_a of 0 and the spectrum remains broadened (*17*). This shift is due to a titration of some group with a very low pK_a, presumably Asp212 (*17*).

Acid titrations of the Tyr83 mutants show that the purple to blue transition is affected in both mutants (Figure 2).

Titration of Y83F. The absorption maximum of the dark-adapted Y83F mutant is at 547 nm near neutral pH, 11 nm blue shifted compared to the dark-adapted WT (Figure 2A). Upon decreasing the pH to 1.5, the absorption maximum undergoes a 21 nm red shift to 568 nm with a pK_a of 2.6, $n = 2$ (Figures 2 and 3A), which is a significantly smaller shift than in the WT. In agreement with this, the absorption changes at 630 nm due to formation of the blue membrane are also much smaller in the Y83F mutant than in the WT (Figure 2B). Examination of the absorption spectra produced by a decrease in pH (Figure 3A) indicates that in Y83F two transitions contribute to this spectral shift. The first transition is characterized by a difference spectrum with its maximum at 620 nm (Figure 3B). It is accompanied by a small red shift of the absorption maximum to ca. 548−550 nm. The pK_a of these absorption changes is ca. 3.7 ($n = 1$) as determined from the absorption increase at 680 nm upon decreasing the pH (Figure 2C, curve 1). The second transition has a difference spectrum with a maximum at 598 nm (Figure 3C); it is accompanied by a larger red shift of absorption maximum to 568 nm (Figure 2A). It has a pK_a of 2.6 ($n = 1.6$) as determined from the plot of absorption changes at 590 nm (Figure 2C, curve 2), the isosbestic point of the first transition. The complex two component purple to blue transition in Y83F is most likely caused by titration of some other acid group, which interacts with Asp85 and affects the pK_a of Asp85. Alternatively it may be due to the separate titration of Asp85 in the all-trans and 13-cis pigments (*44*). In the WT, the second low pH transition is less noticeable, and absorption changes at 630 nm can be reasonably well approximated with a single pK_a of 2.6 ($n = 1.6$). Titration of the Y83F mutant in 75 mM K_2SO_4 and in 150 mM KCl in the pH range from pH 7 to pH 1.5 gave similar results.

Titration of Y83N. Decreasing the pH of a dark-adapted suspension of the Y83N mutant from 6.7 to 3.0 causes formation of the blue membrane, which is accompanied by an almost 30 nm shift of the absorption maximum, from 555 to 584 nm (Figures 2A and 4A). The difference spectrum of this transition has maximum at 630 nm, which is close to that for the WT (632 nm); the pK_a of this transition is 3.4 ($n = 0.8$) (Figure 4B). At lower pH, the absorption maximum shifts back to shorter wavelengths (552 nm) (Figure 2A) with the pK_a 2.5 ($n = 1$). The spectrum remains broad. The difference spectrum of this transition has its maximum at 620 nm (Figure 4C). In the WT, a similar transition occurs below pH 2 with a pK_a of about 0 (*17*). It was attributed to protonation of Asp212 (*17*). On the basis of this, one can suggest that the Y83N mutation causes an increase of the proton affinity of Asp212 by about 2.5 units.

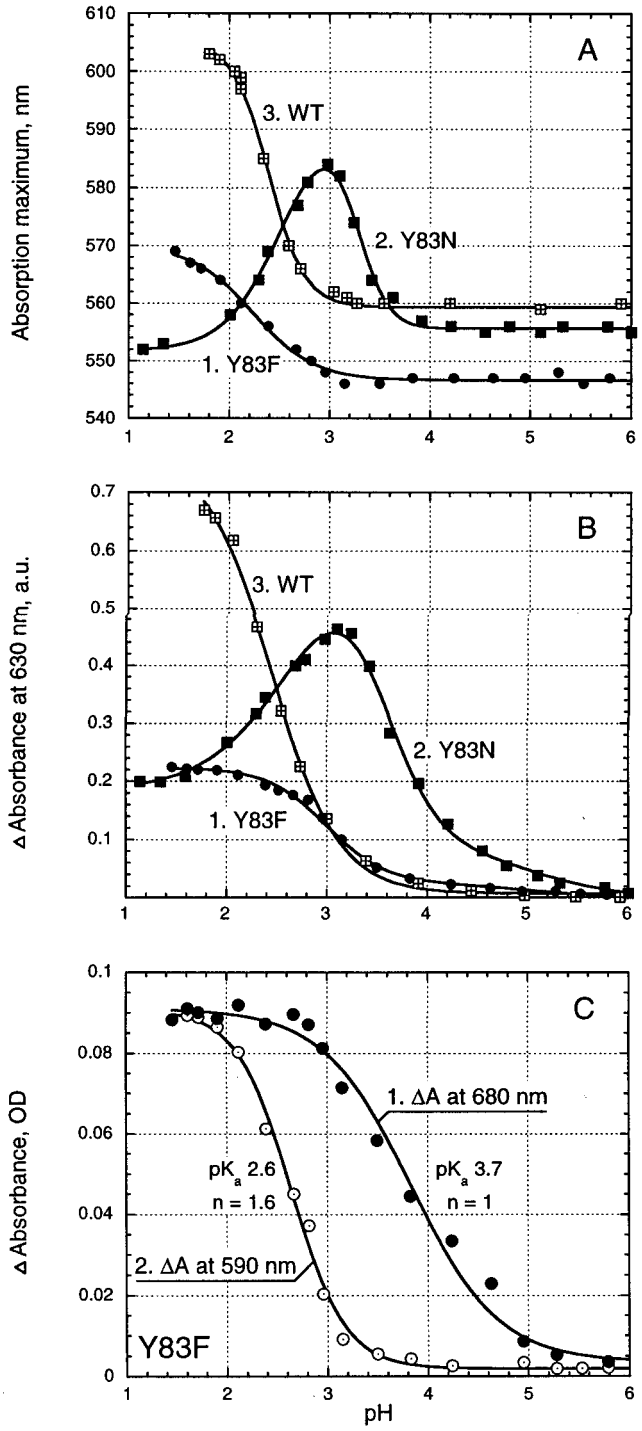

FIGURE 2: Comparison of purple to blue transitions in the Y83F, Y83N mutants and WT. (A) pH dependence of absorption maximum in dark adapted suspensions of Y83F (1), Y83N (2), and WT (3). K_2SO_4, 75 mM, 20 °C. (B) pH dependence of absorption changes at 630 nm in Y83F (1), Y83N (2), and WT (3). Absorption changes are given for the samples with initial optical density at neutral pH equal to 1. (C) pH dependence of the absorption changes at 680 nm (1) and 590 nm (2) in the Y83F mutant. The ΔA at 680 nm were multiplied by 3.9 to normalize with ΔA at 590 nm in the maximum.

Spectral Transitions at High pH. The Y83F and particularly the Y83N mutation dramatically decrease the stability

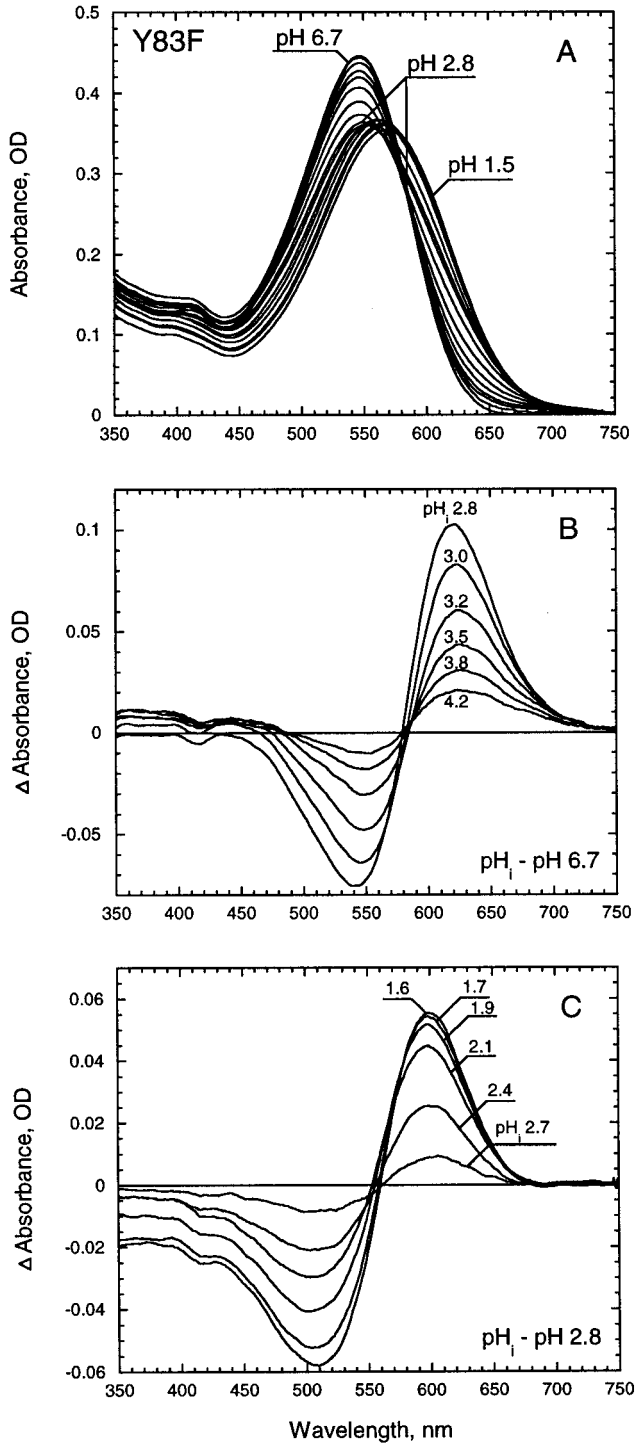

FIGURE 3: (A) Absorption spectra of a suspension of the Y83F mutant over the pH range between 6.7 and 1.5. K_2SO_4, 75 mM, 20 °C. (B) Difference absorption spectra over the pH range between 6.7 and 2.8. Spectra were obtained as a difference between the spectrum taken at the given pH_i and one taken at pH 6.7. (C) Difference absorption spectra in the pH range between 2.8 and 1.6. Spectra were obtained as a difference between spectrum taken at the given pH_i and one taken at pH 2.8.

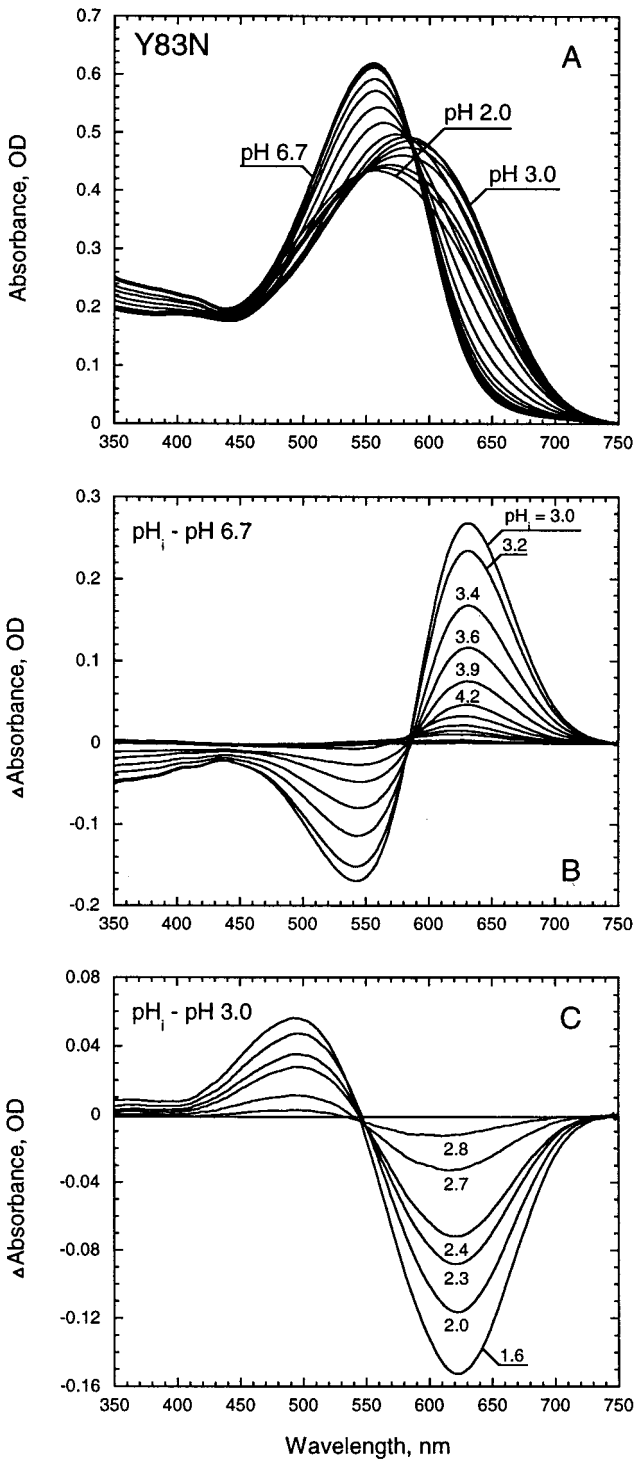

FIGURE 4: (A) Absorption spectra of a suspension of the Y83N mutant over pH range between 6.7 and 2.0. K_2SO_4, 75 mM, 20 °C. (B) Difference absorption spectra over the pH range between 6.7 and 3.0. Spectra were obtained as a difference between spectrum taken at given pH_i and one taken at pH 6.7. (C) Difference absorption spectra over the pH range between 3.0 and 1.6. Spectra were obtained as a difference between spectrum taken at given pH_i and one taken at pH 3.0.

of the pigment at high pH. The Tyr83 mutants exhibit a large decrease in the fraction of functionally active purple form at high pH. This is due to its transformation into the inactive blue-shifted species absorbing at 480 nm, P480 (*45*) (Figure 5A). The pK_a of this transition is 8.2 in Y83F (Figure 5B, curve 1). An analogous transition occurs in the Y83N mutant with a pK_a of 8.8 (Figure 5B, curve 2). Comparison with the WT (Figure 5B, curve 3) shows that the fraction of the pigment converted into P480 at pH 10 is much larger for the Tyr83 mutants than for the WT, particularly for the Y83N mutant. It was proposed earlier (*46*) that partial transition into P480 might reflect deprotonation of the proton release group in the initial unphotolyzed state. If this holds for the

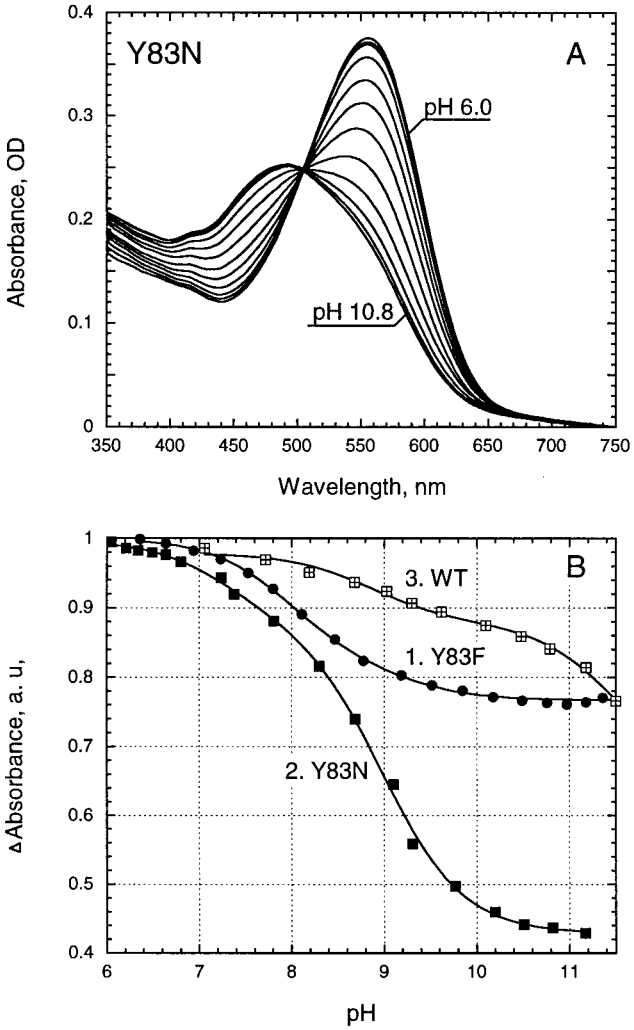

FIGURE 5: Formation of the photochemically inactive species P480 in the Tyr83 mutants and WT. (A) Absorption spectra of the suspension of the Y83N mutant over the pH range between 6.0 and 10.8. K_2SO_4, 75 mM, 20 °C. (B) pH dependence of absorption changes due to formation of P480 in the Y83F (1), Y83N (2) and WT (3). To illustrate the relative level of the formation of P480 for each pigment, absorption changes at 570 nm at given pH were normalized to the maximal optical density in initial spectrum taken at pH 6.0 for each pigment.

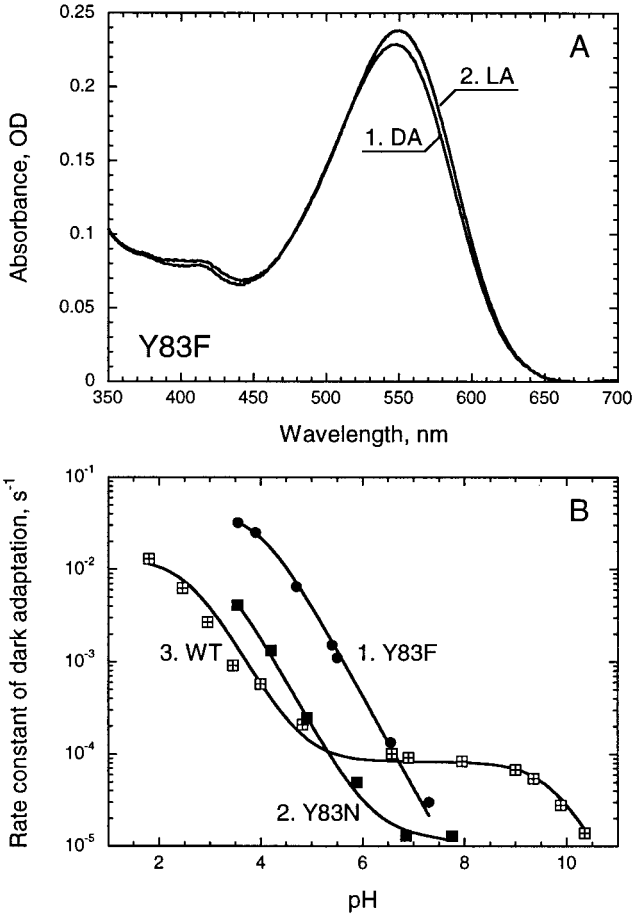

FIGURE 6: (A) Absorption spectra of a dark adapted (1) and light-adapted (2) suspension of the Y83F mutant at pH 6.8. K_2SO_4, 75 mM, 20 °C. (B) pH dependence of the rate constant of dark adaptation in Y83F (1), Y83N (2), and WT (3) at 20 °C.

Y83 mutants, then one may assume that the pK_a of PRC is about 8.8 in the Y83N mutant and 8.2 in the Y83F mutant.

pH Dependence of the Rate Constant of Dark Adaptation. The rate constant of thermal isomerization of all-trans pigment to a 13-cis one is proportional to the fraction of protonated Asp85 over a wide pH range (*35*, *36*, *44*). The pH dependence of the rate constant of dark adaptation can be used to determine the pK_a of the PRC in the ground state and the strength of its interaction (coupling) with the primary proton acceptor Asp85. It can be also used as an approach to explore the interaction of Asp85 with other ionizable groups in BR (*15*, *17*, *27*, *35*, *37*, *47*, *48*).

Light and Dark Adaptation in Y83F Is Greatly Altered. The absorption spectrum of light-adapted Y83F is shown in Figure 6 A. Its maximum (550 nm) is about 20 nm blue shifted compared to the WT. Only a 3 nm blue shift in the absorption maximum is observed upon dark adaptation (versus 10 nm in the WT). The maximum in the "light-adapted minus dark-adapted" difference spectrum is at 565 nm, which is blue shifted 20 nm compared to the difference spectrum of the WT. The amplitude of the "light-adapted minus dark-adapted" difference spectrum in Y83F is ca. 5 times smaller than in the WT. This indicates that less pigment undergoes the 13-cis → all-trans photoisomerization upon light adaptation of Y83F or that the difference in the absorption spectra of 13-cis and all-trans pigments is smaller in Y83F than in the WT.

The kinetics of dark adaptation were followed by measuring the absorption changes at 565 nm in the dark after light adaptation of the sample by illuminating at 450−550 nm. At pH 6.6, the rate constant of dark adaptation (k_{da}) in Y83F is close to that in the WT. However, the pH dependence of the rate constant is quite different from that in the WT. At pH 5.6, in the Y83F mutant the rate constant is almost an order of magnitude larger than at pH 6.6, whereas in the WT it stays the same (Figure 6B). Unlike the WT, the pH dependence of the rate constant of dark adaptation in Y83F does not show a plateau between pH 5 and 7. The k_{da} in Y83F linearly decreases upon increasing the pH from 5 to 7.3. This indicates that the interaction (coupling) of Asp85 with the PRC, which is responsible for the plateau in the WT (*27*), is strongly reduced or eliminated in Y83F.

Dark Adaptation of Y83N. The spectral changes upon light and dark adaptation of the Y83N mutant are much larger than in Y83F and are similar to those in the WT (data not shown). However, the pH dependence of the rate constant

of dark adaptation is different. At neutral pH, the rate of dark adaptation in the Y83N mutant is much slower than for the WT (Figure 6B). At pH 6.9, 20 °C, the time constant of the dark adaptation of the Y83N mutant is about 21 h versus 3 h in the WT. The pK_a of the pH dependence of the rate constant in the low pH range is slightly higher in Y83N than in the WT (3.3 versus 2.6), in agreement with the increased pK_a of Asp85 in Y83N observed in the purple to blue transition (Figure 2). The most important difference in the pH dependencies of the rate constant of dark adaptation in the Y83N mutant and in the WT is that in the Y83N mutant the plateau starts at higher pH. Because of conversion of the pigment into P480 at alkaline pH, we could not obtain reliable data on the rate constants of dark adaptation in the Y83N mutant at pH above 8. This precludes us from determining whether a transition in the pH dependence of the rate constant of dark adaptation at high pH is present in the Y83N mutant [similar to one seen in the WT with a pK_a of 9.7 (*27*)]. However, earlier we have noticed a correlation between the pK_a of partial transformation of the pigment into P480 and the pK_a of the PRC in the initial state (*46*). Assuming that this holds for the Y83N mutant, one may expect that the pK_a of the PRC in the unphotolyzed state of Y83N is about 8.8−9.

The fit of the pH dependence of dark adaptation with the model, which assumes coupling between Asp85 and the PRC, shows that the point on the curve where the plateau starts (pH 4.8 in the WT) corresponds to the pK_a of the PRC when Asp85 is protonated (*27*). In the Y83N mutant, this point is shifted to pH 6.2, indicating that the pK_a of the PRC when Asp85 is protonated is elevated in Y85N by about 1.4 units compared to the pK_a in the WT. From this one would expect an elevated pK_a of the PRC when the pigment is in the M state (which is exactly what is observed, see below). The pH dependence of the rate constant of dark adaptation and the pH dependence of transformation into P480 indicate that in Y83N mutant the coupling strength between Asp85 and the PRC is reduced by about 2 pK units, from 4.9 in the WT (*15*) to about 2.7. This decrease in the coupling strength would likely reduce the influence of deprotonation of the PRC on the kinetics of M rise at high pH (see below).

These estimates are valid if the plateau in Y83N is caused by the interaction of Asp85 and the PRC as in the WT (*27*). However, there is an alternative explanation for the plateau in the pH dependence of the rate constant of dark adaptation in Y83N. The rate of thermal isomerization, k_{da}(pH), is determined by two terms (*15*, *47*):

$$k_{da}(\mathrm{pH}) = k_{da}^{bm} f_{bm}(\mathrm{pH}) + k_{da}^{pm} f_{pm}(\mathrm{pH}) \qquad (1)$$

The first one is the product of the rate constant of thermal isomerization in the blue membrane, k_{da}^{bm}, and the fraction of protonated Asp85, f_{bm}(pH). The second is a product of the rate constant of isomerization in the purple membrane (where Asp85 is deprotonated) and fraction of purple membrane (*15*, *27*, *35*, *36*, *47*). At low and neutral pH, the first term dominates. At high pH where the fraction of blue membrane decreases below 0.01%, the rate of isomerization in the purple membrane might become faster than the rate of isomerization through the transient protonation of Asp85. Under these conditions, the rate would be equal to k_{da}^{pm} and would not change upon further increases in pH, as was observed for E204Q (*37*) and R82H (*47*). One cannot exclude that the plateau in k_{da}(pH) that we see in Y83N at pH >6 corresponds to this basal rate of the chromophore isomerization in the purple membrane. However, this rate constant in Y83N is 3.3 times larger than the basal rate constant found for the R82H mutant (10^{-5} versus 3×10^{-6} s^{-1}) (*47*). This implies that the plateau, in the pH dependence of rate constant of dark adaptation in Y83N, is most likely due to the coupling between Asp85 and the PRC rather than reaching the basal rate of isomerization at high pH. The presence of the fast proton release following M is in agreement with this interpretation.

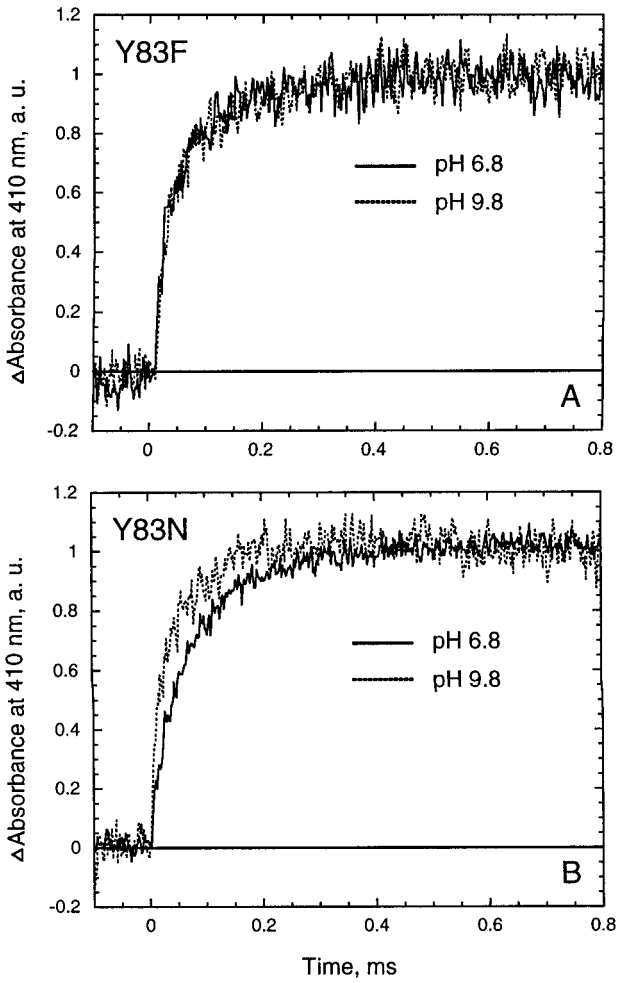

FIGURE 7: Kinetics of the formation of the M intermediate in Tyr83 mutants at different pHs. (A) Formation of the M intermediate in the Y83F mutant at pH 6.8 and 9.8. (B) Formation of the M intermediate in the Y83N mutant at pH 6.8 and 9.8.

Photocycle Reactions in the Y83F and Y83N Mutants. At pH 6.8, the time constant of M formation for the Y83F mutant is 46 μs and for the Y83N mutant is about 80 μs. At higher pH no substantial increase in the rate constant of M formation is seen in Y83F (Figure 7A). A small increase (about 1.8-fold) in the rate of M rise is observed in Y83N (Figure 7B). The pK_a of this transition is about 9. This is different from the WT in which a dramatic increase in the rate of M formation is observed (*45*, *49*−*51*). The increase in the rate of M formation in the WT is caused presumably by deprotonation of the PRC in the initial state at elevated pHs, which results in an increased proton affinity of Asp85 and faster M formation (*17*, *52*). The much smaller increase

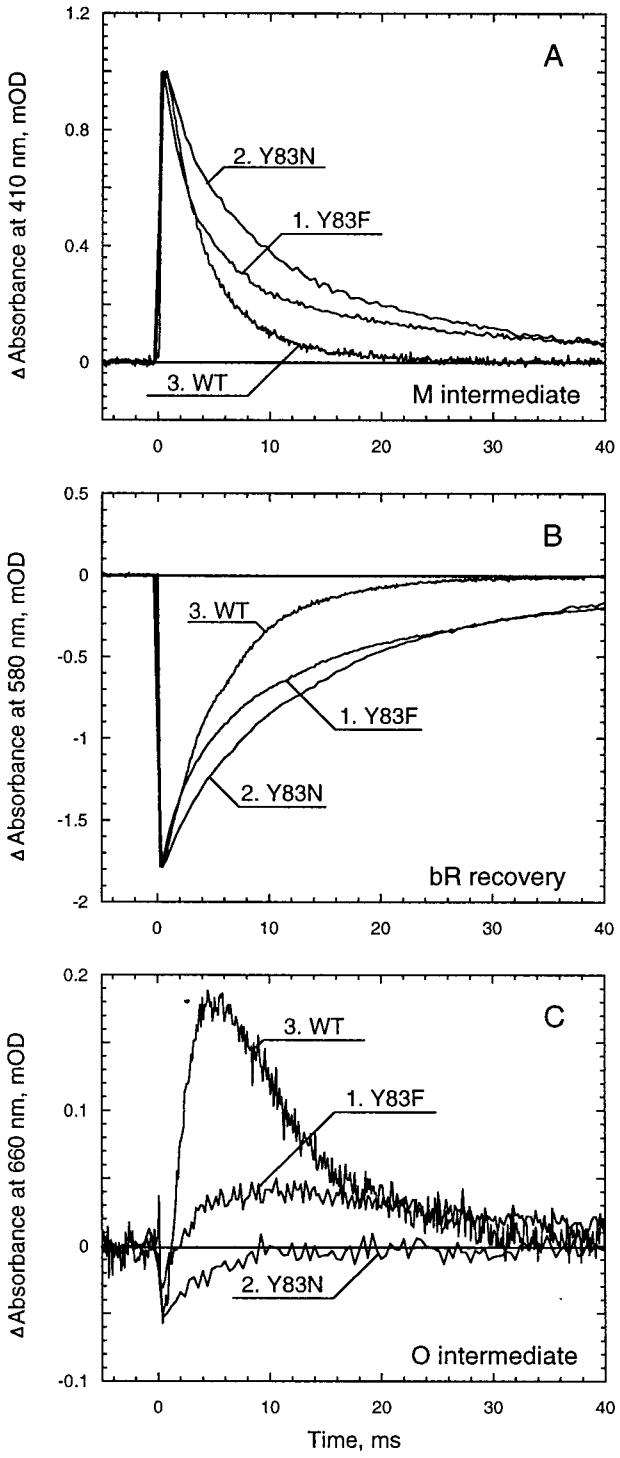

FIGURE 8: Kinetics of the photocycle in the Tyr83 mutants and WT. (A) Absorption changes at 410 nm. Curves 1−3 represent formation and decay of the M intermediate in the Y83F, Y83N mutants and WT. Absorption changes were normalized at the maximum. (B) Absorption changes at 580 nm. They reflect pigment recovery after illumination. (C) Absorption changes at 660 nm, which show formation and decay of the O intermediate. Absorption changes at 660 and 580 nm were normalized to the amplitude of the M intermediate for each pigment, respectively. pH 6.8, 150 mM KCl, 20 °C.

in the rate of M formation in the Y83N mutant indicates that mutation of Tyr83 results in a decrease of the coupling of the PRC with Asp85.

The amount of M formed is maximal at pH 6 in Y83F. It decreases six times upon decreasing the pH to 3 with a pK_a of 4.1. This pK_a is 1.5 units higher than the pK_a of the Asp85 determined from the major component of the purple to blue transition (pK_a of 2.6), which indicates that the yield of M in Y83F is controlled by some low pK_a group different from Asp85 as was observed for R82H (*47*). At high pH, the amplitude of M decreases by half with pK_a 8.0 in the Y83F mutant and pK_a 8.5 in the Y83N mutant presumably due to the transition of the pigment into P480.

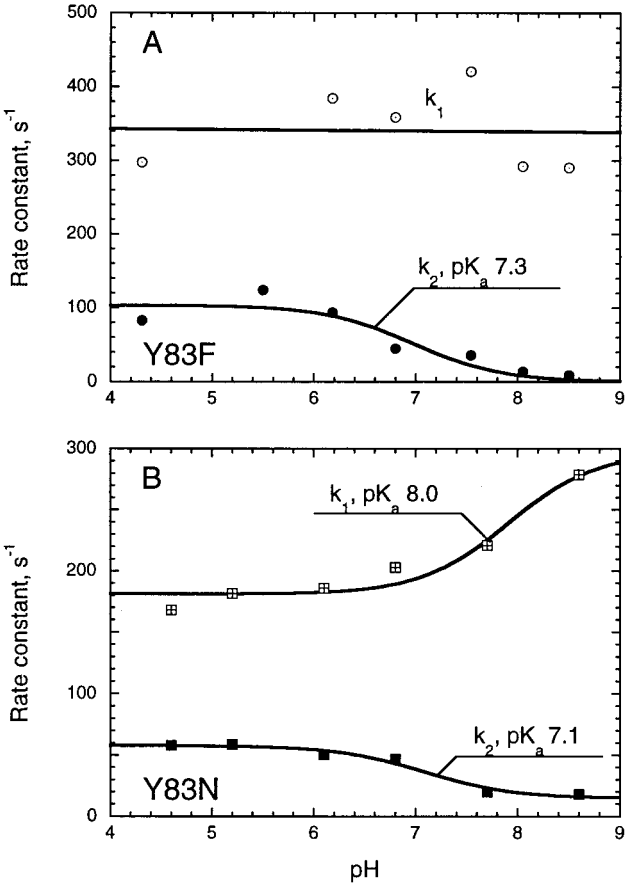

FIGURE 9: (A) pH dependence of the rate constants of the first (k_1) and second (k_2) components of M decay in the Y83F mutant. (B) pH dependence of the rate constants of first (k_1) and second (k_2) components of M decay in the Y83N mutant.

Comparison of light-induced absorption changes at 410, 580, and 660 nm, which represent formation and decay of the M intermediate, BR recovery and formation and decay of the O intermediate, respectively, for the Y83F, Y83N, and WT are shown in Figure 8. They indicate that M decay (Figure 8A) and bR recovery (Figure 8B) are slowed in both mutants compared to the WT.

As in the WT, the kinetics of M decay in Y83F and Y83N can be fitted with two components at neutral pH. In the Y83F mutant (Figure 9A) at pH 6.8, the time constant of the first component of M decay is about 3 ms and does not change significantly with pH. The time constant of the second component is 10 ms at pH 6. It decreases with a pK_a of 7.3 upon increasing the pH. This pK_a most likely corresponds to the pK_a of Asp96 in N during proton uptake (*15*, *36*). In the Y83N mutant (Figure 9B) at pH 6.1, the time constant of the first component is 5 ms (60% of the amplitude of M decay) and of the second component is about 20 ms. At higher pHs, the rate constant of the first component of M decay increases with a pK_a of 8. A similar increase takes

place in the WT with pK_a close to 9. It can be tentatively connected to the deprotonation of the PRC in the ground state. The rate constant of the second component of M decay in Y83N decreases with the pK_a of 7.1.

The recovery of the initial absorbance at 580 nm is biphasic at pH 6.8 (Figure 8B). In the WT, the fraction of the fast phase (5 ms) is much larger than that of the slow phase (12 ms) (90% versus 10%). In both mutants, the fraction of the slow phase is increased 5−7-fold compared to the WT. In Y83F, the fast 5 ms phase comprises 40%, whereas 60% of the total is due to the slow (25 ms) phase. In Y83N, fast 4.8 ms phase accounts for 30% and slow, 19 ms phase, for 70% of the total.

In the Y83F mutant the maximum amount of the O intermediate (Figure 8C, curve 1) is about 3 times less than in the WT (Figure 8C, curve 3) despite the lower rate constant for O decay. Upon increasing the pH, the fraction of O decreases with pK_a 7.4 in Y83F similar to that in WT. A surprising feature of the Y83N mutant is almost complete absence of the O intermediate at pH 6.8 (Figure 8C, curve 2) and even at pH 4.5.

Light-Induced Proton Release and Uptake in the Y83F and Y83N Mutants. The kinetics of light-induced changes of the concentration of hydrogen ions in a suspension of the Y83F and Y83N mutants were measured with the pH sensitive dye pyranine. Addition of a 10 mM buffer eliminated the dye signal.

The kinetics of proton release is pH dependent around neutral pH both in Y83F and Y83N mutant. Unlike in the WT, no fast proton release can be seen in Y83F at pH 6.3 (Figure 10 A). The light-induced proton release in the Y83F mutant at pH 6.3 occurs with the time constant of ca. 30 ms which is close to the 21−25 ms decay of the O intermediate.

At pH >7, both fast and slow components of proton release are observed (Figure 10B) in agreement with the data of Brown (*53*). The pK_a of the switch between fast and slow proton release is about 7.2, which is ca. 1.5 pK units higher than in WT. This pK_a presumably can be attributed to a PRC in M.

The kinetics of proton uptake in the Y83F mutant is similar to that in the WT (Figure 10A). The time constant of proton uptake is about 6 ms, and it increases at high pH with pK_a approximately 7.5, which is close to that in the WT (7.5−7.7) (*54*). This pK_a presumably is the pK_a of Asp96 (*36*, *55*) in the state where its accessibility to the cytoplasmic surface is increased in order to speed up proton uptake and its reprotonation (*15*).

Light-induced proton release and uptake in a suspension of the Y83N mutant is shown in Figure 10C. As in the Y83F mutant, in Y83N, there is fast proton release at pH 7.8, and the kinetics of proton release shows strong pH dependence (*56*). At pH 7.8, the time constant of light-induced proton release is 2.8 ms. It is followed by proton uptake with time constant 33 ms. At pH 6.6, no fast proton release occurs. At this pH, the light-induced pyranine signal consists of two components: proton uptake with time constant 5 ms and slow proton release with time constant ca. 50 ms.

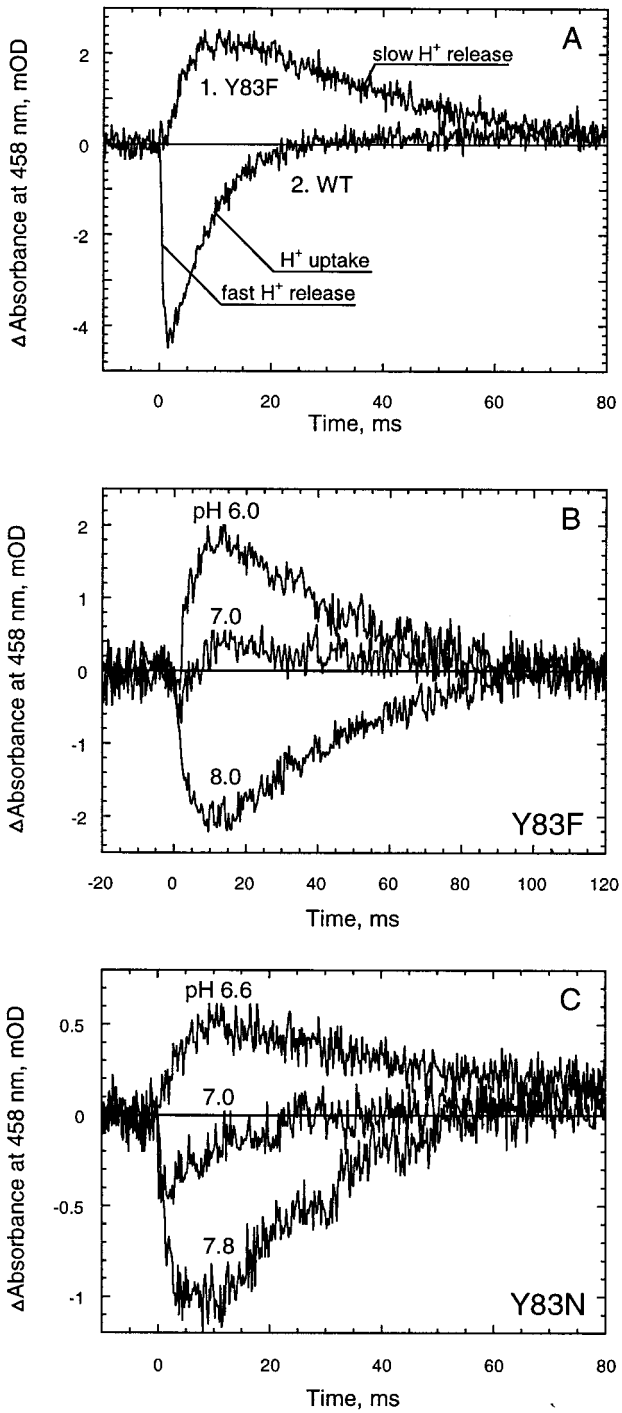

FIGURE 10: (A) Light-induced pyranine signal at 458 nm in 1, Y83F; 2, WT. pH 6.3, 150 mM KCl. An increase of absorbance is caused by proton uptake; a decrease of absorbance is caused by proton release from a protein. (B) Light-induced pyranine signal in a suspension of the Y83F mutant at different pHs. (C) Light-induced pyranine signal in a suspension of the Y83N mutant at different pHs.

DISCUSSION

Effects of the Y83F and Y83N Mutations on Light-Induced Proton Release. In WT bacteriorhodopsin, light-induced proton release precedes proton uptake at neutral pH. At low pH, proton release occurs after uptake (*22*, *57*). The transition between the two modes of proton release, "fast" and "slow" occurs with a pK_a of 5.8 (*22*), which can be assigned to the pK_a of the PRC in the M intermediate. Fast proton release at neutral pH has a time constant of about 80−100 μs and approximately coincides with the formation of the M intermediate (*58*−*62*).

In the Y83F mutant, fast proton release is inhibited below pH 7 (Figure 10, panels A and B). This, and also the lack of the pH dependence of M formation (Figure 7A) as the pH is increased from 6 to 10 (a region where the WT shows a dramatic increase of the rate of M formation) and the altered pH dependence of dark adaptation with no plateau (Figure 6B, curve 1), indicates that the coupling between PRC and Asp85 is greatly weakened in theY83F mutant so that protonation of Asp85 cannot cause fast proton release following the formation of the M intermediate at pH lower than 7.

Not only is the pK_a for fast proton release elevated in Y83F, but proton release from Asp85 at the end of the photocycle occurs very slowly with a rate similar to that in the E204Q mutant. The dramatic slowing of proton release from Asp85 during the O → BR transition in Y83F indicates that the Y83F mutation hinders deprotonation of Asp85 and the proton transfer to the surface of the membrane. Substitution of Tyr83 with a nonpolar Phe (and also with Asn) apparently disrupts a chain of hydrogen-bonded residues presumably in the site close to Glu194 and creates a barrier for proton transfer from Asp85 to the PRC. These data indicate that the hydroxyl group of Tyr83 is an important component of the complex of residues involved in proton release. The question arises whether Tyr83 itself could be a source of the proton released during the L → M transition. The Y83F and Y83N mutants show fast light-induced proton release that precedes uptake at pH above 7 (Figure 10, panels B and C). This indicates that Tyr83 is not the major (or the only) source of a proton. The data suggest that the Y83F and Y83N mutations results in an increase in the pK_a of the PRC in M rather than in disabling the PRC completely.

The time constant for proton release in the Y83 mutants as measured with pyranine is about 3 ms. This is longer than in the WT (less than 0.8 ms if measured with pyranine and about 0.1 ms if measured with surface bound fluorescein) (*60*, *62*). This increase in the time constant of proton release correlates with the proposed increase in the pK_a of the PRC because the rate constant for deprotonation of a group depends on the pK_a of the group. In water $k_d = 2 \times 10^{(10-pK_a)}$ (*63*). This formula can be applied to the PRC in BR. A perfect correlation between the pK_a of PRC in WT (5.8 in M) and k_d ($1/k_d = 80$ μs) is achieved when the coefficient 2 is replaced with 0.7. Increase in the time constant of proton release from 80 μs to 3 ms corresponds to an increase in the pK_a of the PRC in M by about 1.5 p*K* units, which agrees fairly well with the experimental value for the increase of 1.4−1.5 p*K* units obtained from the pH dependence of proton release.

Mutations of Tyr83 to Phe and Asn Reduce Coupling between Asp85 and the PRC. In the WT, the primary proton acceptor Asp85 exhibits a complex two component titration curve, which was explained by the interaction (coupling) of Asp85 and the PRC. Deprotonation of the latter with pK_a ca. 9.7 results in the increase in the pK_a of Asp85 by almost 5 p*K* units (*27*). The evidence for this was obtained from a direct titration of Asp85 and from the pH dependence of the rate constant of thermal isomerization, which is proportional to the fraction of protonated Asp85 (*17*, *27*, *35*). The functional significance of this coupling is that it provides a "mechanism" for the proton to be released extracellularly upon protonation of Asp85 by reducing the pK_a of the PRC. In Y83F, the coupling between Asp85 and the PRC is greatly weakened (the pK_a of fast proton release is elevated by 1.5 p*K* units, no pH dependence of M rise, and no plateau in the pH dependence of the rate constant of dark adaptation are observed).

The linkage between the PRC and Asp85 is greatly decreased also in Y83N. The pH dependence of the rate constant of dark adaptation in Y83N (Figure 6B, curve 2) indicates that the pK_a of the PRC, when Asp85 is protonated, is about 6.2, which is 1.4 units higher than in the WT (4.8). The pK_a of the PRC in the unphotolyzed state of Y83N when Asp85 is deprotonated is decreased from about 9.7 in the WT to ca. 9 in Y83N as one can assume from the pH dependence of transition into P480 (Figure 5). Thus, the coupling strength is reduced from 4.9 in the WT (*44*, *47*) to about 2.7 in Y83N.

The pH dependence of the kinetics of M formation (Figure 7) is in agreement with the decreased coupling between proton affinity of Asp85 and the protonation state of the PRC. The Y83N mutant shows only a small increase in the rate of M formation at high pH (pK_a around 9). These data clearly indicate that Tyr83 is important in decreasing the pK_a of the PRC during the photocycle and in keeping it high in the unphotolyzed state. It is likely that the hydrogen bond between the hydroxyl of Tyr83 and the carboxyl of Glu194 (Figure 1B), which is formed (or strengthening) during the BR to M transition (*33*, *34*), is important in causing a decrease of the pK_a of the PRC in M.

Mutation of Tyr83 Slows Recovery of the Initial State in the Photocycle and Affects the Accumulation and Decay of the O Intermediate. A remarkable feature of the Y83N mutant is the almost complete absence of the O intermediate (Figure 8C). In the Y83F mutant, the O intermediate is formed but the amount is three times less than in the WT. The N → O transition is apparently slowed in the photocycle of the Y83N mutant and the N ↔ O equilibrium is strongly shifted toward N. Both Asp96 and Asp85 are protonated in the O intermediate (*64*, *65*). A possible explanation for the decreased amount of O could be a decreased rate of Asp96 reprotonation and/or an increased rate of Asp85 deprotonation. As suggested earlier (*36*) and observed recently for the E194Q mutant (*66*), the deprotonation of Asp85 might occur already in the N intermediate. If protonated Asp85 facilitates isomerization of the chromophore during the N ↔ O_1 ↔ O_2 transitions (*11*), as it does during thermal all-trans ↔ 13-cis isomerization (*27*, *35*, *44*), then the early deprotonation of Asp85 in N could explain decreased amount of the O intermediate and decreased rate of the initial state recovery in the photocycles of Y83F and Y83N mutant. According to Dioumaev et al. (*67*), Asp212 might be an intermediate proton acceptor from Asp85. If so, then an increase in the pK_a of Asp212 would facilitate fast deprotonation of Asp85 in the second half of the photocycle and thus reduce amount of the O intermediate. An alternative explanation for a decreased amount of O is that the N ↔ O equilibrium is strongly shifted toward N, particularly in the Y83N mutant.

Tyr83 Is Important for Maintaining Functionally Active Purple Form of BR at High pH. Certainly, one of the functions of Tyr83 in BR is maintaining the functionally active purple form of BR at high pH. In both Y83N and Y83F mutants, increased amount of the functionally inactive blue shifted form called P480 (*45*, *68*) is observed at elevated

pHs (Figure 5). Partial transformation into P480 was observed also for the WT at pH 10 but in much smaller amounts (*45*). The origin of P480 is unclear. It was suggested that partial transformation of BR into P480 might be facilitated by deprotonation of the PRC (*46*). It could be that deprotonation of the PRC decreases the pK_a of some other residue, presumably Asp96, deprotonation of which leads to the formation of P480. Tyr83 (in helix C) is hydrogen bonded with Trp189 (in helix F) in the initial BR state (*7*). Elimination of this bond by mutation might affect the pK_a of the PRC and Asp96 in the ground state.

Does Tyr83 Deprotonate at pH around 9.7 in the WT? An interesting question is whether Tyr83 could be the group that deprotonates in the dark at high pH and serves as the light-induced source of the proton that is released upon M formation. The most straightforward interpretation of the data on Y83F and Y83N mutants does not support this possibility. The observation that proton release precedes proton uptake at pH 8 (Figure 10, panels B and C) indicates that the PRC is functional in both in Y83F and Y83N though with an elevated pK_a. Tyr83 cannot be the source (or at least the major source) of the released proton in these mutants. A small increase in the rate constant of M formation at high pH, the presence of a plateau in the pH dependence of dark adaptation, the formation of P480 are all consistent with the deprotonation of the PRC with pK_a around 8.8 in the ground state of Y83N. That would imply that Tyr83 mainly controls the pK_a of the PRC, or contributes to the system of hydrogen bonds that constitutes the PRC, but is not a main source of the proton released from the PRC. The Tyr83 mutations apparently disrupt the hydrogen bonding network at the extracellular channel which results in a decreased initial pK_a of the PRC and strong delay of proton release at low pH.

In conclusion, study of Y83F and Y83N mutants revealed a large impact of these mutations on the kinetics of light-induced proton release. The results point to the important role of a hydrogen bonding of Tyr83 with Glu194 and Trp189 in fast light-induced proton transfer in the extracellular channel, in the rate of photocycle turnover and in the functional stability of the protein at high pH.

ACKNOWLEDGMENT

The authors thank James Beall (MUSC, Department of Ophthalmology) for growing the *Halobacterium salinarum* cells and isolation of purple membranes of mutant pigments.

REFERENCES

1. Oesterhelt, D., and Stoeckenius, W. (1973) *Proc. Natl. Acad. Sci. U.S.A. 70*, 2853−2857.
2. Michel, H., and Oesterhelt, D. (1980) *FEBS Lett. 65*, 175−178.
3. Drachev, L. A., Kaulen, A. D., Khitrina, L. V., and Skulachev, V. P. (1981) *Eur. J. Biochem. 117*, 461−470.
4. Henderson, R., Baldwin, J. M., Ceska, T. A., Zemlin, F., Beckmann, E., and Downing, K. H. (1990) *J. Mol. Biol. 213*, 899−929.
5. De Groot, H. J. M., Harbison, G. S., Herzfeld, J., and Griffin, R. G. (1989) *Biochemistry 28*, 3346−3353.
6. Maeda, A., Sasaki, J., Shichida, Y., and Yoshizawa, T. (1992) *Biochemistry 31*, 462−467.
7. Luecke, H., Schobert, B., Richter, H.-T., Cartailler, J.-P., and Lanyi, J. K. (1999) *J. Mol. Biol. 291*, 899−911.
8. Lozier, R. H., Bogomolni, R. A., and Stoeckenius, W. (1975) *Biophys. J. 15*, 955−963.
9. Mathies, R. A., Lin, S. W., Ames, J. B., and Pollard, W. T. (1991) *Annu. Rev. Biophys. Biophys. Chem. 20*, 491−518.
10. Rothschild, K. J. (1992) *J. Bioenerg. Biomembr. 24*, 147−167.
11. Ebrey, T. G. (1993) in *Thermodynamics of Membrane Receptors and Channels* (Jackson, M. B., Ed.) pp 353−387, CRC Press, Boca Raton, FL.
12. Lanyi, J. K. (1993) *Biochim. Biophys. Acta 1183*, 241−261.
13. Lanyi, J. K., and Váró, G. (1995) *Isr. J. Chem. 35*, 365−385.
14. Chizhov, I., Chernavskii, D. S., Engelhard, M., Mueller, K.-H., Zubov, B. V., and Hess, B. (1996) *Biophys. J. 71*, 2329−2345.
15. Balashov, S. P. (2000) *Biochim. Biophys. Acta 1460*, 75−94.
16. Honig, B., Ottolenghi, M., and Sheves, M. (1995) *Isr. J. Chem. 35*, 429−446.
17. Balashov, S. P., Govindjee, R., Imasheva, E. S., Misra, S., Ebrey, T. G., Feng, Y., Crouch, R. K., and Menick, D. R. (1995) *Biochemistry 34*, 8820−8834.
18. Braiman, M. S., Dioumaev, A. K., and Lewis, J. R. (1996) *Biophys. J. 70*, 939−947.
19. Braiman, M. S., Mogi, T., Marti, M., Stern, L. J., Khorana, H. G., and Rothschild, K. J. (1988) *Biochemistry 27*, 8516−8520.
20. Metz, G., Siebert, F., and Engelhard, M. (1992) *FEBS Lett. 303*, 237−241.
21. Siebert, F., Mäntele, W., and Kreutz, W. (1982) *FEBS Lett. 141*, 82−87.
22. Zimányi, L., Váró, G., Chang, M., Ni, B., Needleman, R., and Lanyi, J. K. (1992) *Biochemistry 31*, 8535−8543.
23. Heberle, J., Oesterhelt, D., and Dencher, N. A. (1993) *EMBO J. 12*, 3721−3727.
24. Brown, L. S., Sasaki, J., Kandori, H., Maeda, A., Needleman, R., and Lanyi, J. K. (1995) *J. Biol. Chem. 270*, 27122−27126.
25. Balashov, S. P., Imasheva, E. S., Ebrey, T. G., Chen, N., Menick, D. R., and Crouch, R. K. (1997) *Biochemistry 36*, 8671−8676.
26. Dioumaev, A., Richter, H.-T., Brown, L. S., Tanio, M., Tuzi, S., Saito, H., Kimura, Y., Needleman, R., and Lanyi, J. K. (1998) *Biochemistry 37*, 2496−2506.
27. Balashov, S. P., Imasheva, E. S., Govindjee, R., and Ebrey, T. G. (1996) *Biophys. J. 70*, 473−481.
28. Rammelsberg, R., Huhn, G., Lübben, M., and Gerwert, K. (1998) *Biochemistry 37*, 5001−5009.
29. Hutson, M. S., Alexiev, U., Shilov, S. V., Wise, K. J., and Braiman, M. S. (2000) *Biochemistry 39*, 13189−13200.
30. Wang, J., and El-Sayed, M. A. (2001) *Biophys. J. 80*, 961−971.
31. Landau, E. M., and Rosenbusch, J. P. (1996) *Proc. Natl. Acad. Sci. U.S.A. 93*, 14532−14535.
32. Belrhali, H., Nollert, P., Royant, A., Menzel, C., Rosenbusch, J. P., Landau, E. M., and Pebay-Peyroula, E. (1999) *Structure 7*, 909−917.
33. Luecke, H., Schobert, B., Richter, H.-T., Cartailler, J.-P., and Lanyi, J. K. (1999) *Science 286*, 255−260.
34. Sass, H. J., Büldt, G., Gessenich, R., Hehn, D., Neff, D., Schlesinger, R., Berendzen, J., and Ormos, P. (2000) *Nature 406*, 649−653.
35. Balashov, S. P., Govindjee, R., Kono, M., Imasheva, E., Lukashev, E., Ebrey, T. G., Crouch, R. K., Menick, D. R., and Feng, Y. (1993) *Biochemistry 32*, 10331−10343.
36. Balashov, S. P., Lu, M., Imasheva, E. S., Govindjee, R., Ebrey, T. G., Chen, Y., Crouch, R. K., and Menick, D. R. (1999) *Biochemistry 38*, 2026−2039.
37. Richter, H.-T., Brown, L. S., Needleman, R., and Lanyi, J. K. (1996) *Biochemistry 35*, 4054−4062.
38. Mukohata, Y., Ihara, K., Tamura, T., and Sugiyama, Y. (1999) *J. Biochem. 125*, 649−657.
39. Béjá, O., Aravind, L., Koonin, E. V., Suzuki, M., Hadd, A., Nguyen, L. P., Jovanovich, S. B., Gates, C. M., Feldman, R. A., Spudich, J. L., Spudich, E. N., and DeLong, E. F. (2000) *Science 289*, 1902−1906.
40. Ball, L. E., Oatis, J. E., Jr., Dharmasiri, K., Busman, M., Wang, J., Cowden, L. B., Galijatovic, A., Chen, N., Crouch, R. K., and Knapp, D. R. (1998) *Protein Sci. 7*, 758−764.

41. Govindjee, R., Misra, S., Balashov, S. P., Ebrey, T. G., Crouch, R. K., and Menick, D. R. (1996) *Biophys. J. 71*, 1011−1023.
42. Fischer, U., and Oesterhelt, D. (1979) *Biophys. J. 28*, 211−230.
43. Mowery, P. C., Lozier, R. H., Chae, Q., Tseng, Y.-W., Taylor, M., and Stoeckenius, W. (1979) *Biochemistry 18*, 4100−4107.
44. Balashov, S. P., Imasheva, E. S., Govindjee, R., Sheves, M., and Ebrey, T. G. (1996) *Biophys. J. 71*, 1973−1984.
45. Balashov, S. P., Govindjee, R., and Ebrey, T. G. (1991) *Biophys. J. 60*, 475−490.
46. Govindjee, R., Imasheva, E. S., Misra, S., Balashov, S. P., Ebrey, T. G., Chen, N., Menick, D. R., and Crouch, R. K. (1997) *Biophys. J. 72*, 886−898.
47. Imasheva, E. S., Balashov, S. P., Ebrey, T. G., Chen, N., Crouch, R. K., and Menick, D. R. (1999) *Biophys. J. 77*, 2750−2763.
48. Richter, H.-T., Needleman, R., and Lanyi, J. K. (1996) *Biophys. J. 71*, 3392−3398.
49. Kalisky, O., Ottolenghi, M., Honig, B., and Korenstein, R. (1981) *Biochemistry 20*, 649−655.
50. Liu, S. Y. (1990) *Biophys. J. 57*, 943−950.
51. Hanamoto, J., Dupuis, P., and El-Sayed, M. A. (1984) *Proc. Natl. Acad. Sci. U.S.A. 81*, 7083−7087.
52. Misra, S., Martin, C., Kwon, O., Ebrey, T. G., Chen, N., Crouch, R. K., and Menick, D. R. (1997) *Photochem. Photobiol. 66*, 774−783.
53. Brown, L. S. (2000) *Biochim. Biophys. Acta 1460*, 49−59.
54. Balashov, S. P., Lu, M., Ebrey, T. G., Chen, Y., Menick, D. R., and Crouch, R. K. (2001) *Biophys. J. 80*, 604A.
55. Zscherp, C., Schlesinger, R., Tittor, J., Oesterhelt, D., and Heberle, J. (1999) *Proc. Natl. Acad. Sci. U.S.A. 96*, 5498−5503.
56. Imasheva, E. S., Balashov, S. P., Ebrey, T. G., Chen, Y., and Menick, D. R. (2000) *Biophys. J. 78*, 2798Pos.
57. Dencher, N., and Wilms, M. (1975) *Biophys. Struct. Mech. 1*, 259−271.
58. Liu, S. Y., Govindjee, R., and Ebrey, T. G. (1990) *Biophys. J. 57*, 951−963.
59. Kono, M., Misra, S., and Ebrey, T. G. (1993) *FEBS Lett. 334*, 31−34.
60. Heberle, J., and Dencher, N. A. (1992) *Proc. Natl. Acad. Sci. U.S.A. 89*, 5996−6000.
61. Alexiev, U., Marti, T., Heyn, M. P., Khorana, H. G., and Scherrer, P. (1994) *Biochemistry 33*, 13693−13699.
62. Cao, Y., Brown, L. S., Sasaki, J., Maeda, A., Needleman, R., and Lanyi, J. K. (1995) *Biophys. J. 68*, 1518−1530.
63. Gutman, M., and Nachliel, E. (1990) *Biochim. Biophys. Acta 1015*, 391−414.
64. Gerwert, K., Souvignier, G., and Hess, B. (1990) *Proc. Natl. Acad. Sci. U.S.A. 87*, 9774−9778.
65. Zscherp, C., and Heberle, J. (1997) *J. Phys. Chem. B 101*, 10542−10547.
66. Lazarova, T., Sanz, C., Querol, E., and Padrós, E. (2000) *Biophys. J. 78*, 2022−2030.
67. Dioumaev, A. K., Brown, L. S., Needleman, R., and Lanyi, J. K. (1999) *Biochemistry 38*, 10070−10078.
68. Druckmann, S., Ottolenghi, M., Pande, A., Pande, J., and Callender, R. H. (1982) *Biochemistry 21*, 4953−4959.

BI0110138